

## Neutron scattering study of the nucleation and growth process at the pressure-induced first-order phase transformation of RbI

N. Hamaya and Y. Yamada

*Faculty of Engineering Science, Osaka University, Toyonaka, Osaka 560, Japan*

J. D. Axe, D. P. Belanger, and S. M. Shapiro

*Department of Physics, Brookhaven National Laboratory, Upton, New York 11973*

(Received 16 July 1985)

We have studied the kinetics of the NaCl-CsCl phase transformation in RbI at room temperature ( $P_c \cong 3.5$  kbar) and at temperatures down to 200 K by monitoring the time-dependent changes in neutron powder diffraction peaks. Within the interval of temperature studied, the rate of growth of the stable phase increases as  $\Delta P = |P - P_c|$  is increased. The characteristic time of completion of transformation  $t_0(P)$  at room temperature diverges as the pressure approaches  $P_c$  consistent with the form  $\Delta P^{-3/4} \exp[B(\Delta P)^{-2}]$ , predicted by classical theory. At room temperature the observed growth curves for various pressures display a nearly universal shape, consistent with the Kolmogorov model of nucleation and growth, when plotted against a scaled time parameter  $\tau = t/t_0(P)$ . At 240 K the growth curves deviate from the universal shape increasingly with increasing  $\Delta P$ . Moreover, within a single growth curve the deviation becomes more evident in the later stage of growth. These observations can be explained qualitatively by taking into account the effect of stress produced by the volume change associated with the transformation.

### I. INTRODUCTION

In recent years there has been renewed interest in the process of nucleation and growth at first-order phase transformations.<sup>1</sup> A key concept in the modern understanding of these phenomena is that with proper scaling of both space and time, the "pattern" of phase transformation is reduced to a universal form.

The universality appears in time developments of various physical quantities such as the fraction of transformed volume  $X(t)$ , the average domain size  $\bar{R}(t)$ , and the domain-size distribution function  $n(R, t)$ . These quantities are directly related to the Bragg scattering intensity  $I(t)$ , width  $W(t)$ , and scattering function  $S(k, t)$ , obtained from various scattering experiments. The relationships between the observables and the quantities,  $X(t)$ ,  $\bar{R}(t)$ , and  $n(R, t)$  are summarized in Table I. Therefore, reflecting the scaling properties of these quantities, the observed scattering should also exhibit similar scaling properties in terms of time and an inverse length scale. In fact, the scaling laws of the scattering function in spinodal decomposition in binary alloys and in order-disorder transformations have been subjected to extensive theoretic

cal<sup>2</sup> and experimental<sup>3,4</sup> study and now seem to be well established.

The processes of nucleation and growth are also widely observed in reconstructive structural first-order phase transformations. However, there have not been extensive investigations to verify scaling properties in the time development of this type of transformation since the pioneering theoretical works by Kolmogorov<sup>5</sup> and Avrami<sup>6</sup> appeared more than forty years ago. They derived an expression for  $X(t)$ , which was empirically found by Johnson and Mehl,<sup>7</sup> on the basis of simple phenomenological assumptions of nucleation and growth. Where possible, we use this simplified picture of nucleation and growth to extract scaling properties from the experimental results for the time development of structural transformation in RbI.

Many alkali halides transform from the NaCl (*B1*) structure to the CsCl (*B2*) structure at high pressures. In particular, RbI undergoes this transformation at a critical pressure  $P_c \cong 3.5$  kbar at room temperature, which is experimentally accessible with neutron scattering techniques. By observing the time variation of neutron powder diffraction pattern after sudden application of hy-

TABLE I. Relationships between the physical quantities and the observable quantities from a scattering experiment.

Physical quantities	Observables
Fraction of transformed volume $X(t)$	Integrated intensity of Bragg scattering $I(t)$
Average domain size $\bar{R}(t)$	Width of Bragg scattering $W(t)$
Domain-size distribution function $n(R, t)$	Scattering function $S(k, t)^a$

<sup>a</sup> $S(k, t)$  is related to  $n(R, t)$  by  $S(k, t) = \int_0^{R_m} n(R, t) |F(k, R)|^2 dR$ , where  $F(k, R)$  is the scattering form factor of a domain with dimension  $R$  and  $R_m$  is the maximum domain size.

drostatic pressure exceeding  $P_c$ , we can, in principle, directly deduce  $X(t)$ ,  $\bar{R}(t)$ , and  $n(R,t)$ . Of many experimental works devoted to the reconstructive first-order phase transformation of alkali halides, few are concerned with the kinetics.<sup>8-10</sup> Daniels and Skoultschi<sup>9</sup> concluded that for single crystals of RbI the nucleation process depends sensitively on the conditions of the crystal surface. Hamaya and Akimoto<sup>10</sup> suggested that for polycrystalline KCl the transformation is controlled by homogeneous nucleation at pressures not too close to  $P_c$ .

The primary purpose of the present study is to test the scaling hypotheses in this system using neutron scattering technique. Results of the preliminary experiments have been reported previously.<sup>11</sup> We also demonstrate that the completion time of transformation critically "slows down" as the pressure approaches  $P_c$ . This critical behavior is compared with the existing theoretical predictions. Finally, an attempt to observe broadening of the Bragg scattering associated with the transformation is briefly reported.

## II. EXPERIMENTAL TECHNIQUES

The sample of high-purity RbI was purchased from Johnson Matthey Chemicals, Ltd. The largest detected metallic impurity was 40 ppm K. No analysis of ionic impurities was available. The granular sample was dried at 250°C for 2 days to remove water. The sample was then ground and passed through a 800-mesh sieve.

A 0.6-g sample was mounted in an aluminum alloy cell of the type previously described,<sup>12</sup> with He gas as the pressure-transmitting medium. The cell was placed in a cryostat for the low-temperature experiments. The pressure was measured with a Manganin resistor which had been calibrated with a Heise pressure gauge. The relative precision of the resistance measurement ( $\Delta R/R = 3.3 \times 10^{-5}$ ) corresponding to  $\Delta P \approx 1.4$  bars. The accuracy of the pressure measurement is estimated to be better than about 50 bars, set by the accuracy of the Heise gauge (0.5%) and the drift and hysteresis in the Manganin resistor. The temperature was controlled within  $\pm 0.5$  K in a cryostat.

The neutron diffraction measurements were performed at the Brookhaven National Laboratory High Flux Beam Reactor using a two-axis spectrometer equipped with a He-gas-filled multiwire area detector with a resolution of about 1 mm. The detector was located about 1 m from sample, giving about 10° arc of coverage, and its center was set at  $2\theta = 41^\circ$ . An incident neutron wave vector of  $2.66 \text{ \AA}^{-1}$  was obtained by reflection from the (002) planes of a pyrolytic graphite monochromator. Under these conditions it was possible to observe simultaneously Debye-Scherrer peaks from both the high- and low-pressure phases. The peaks observed were the (200) reflection of the NaCl-type ( $B_1$ ) structure and the (110) reflection of the CsCl type ( $B_2$ ). An observed two-dimensional diffraction pattern was reduced to the one-dimensional pattern by integrating the measured counts along the direction perpendicular to the scattering plane. Sufficient intensity was obtained with counting times of the order of 30 sec. The resolution was measured at the (200)<sub>B1</sub> reflec-

tion to be  $0.031 \text{ \AA}^{-1}$  full width at half maximum. The time development of the diffraction pattern was observed after sudden increase (reduction) of hydrostatic pressure from  $P < (>) P_c$  to  $P > (<) P_c$  at a constant temperature. Since the transformation of RbI accompanies a fractional volume change of about 0.13 between two structures, we would expect a change in the free-cell volume and thus in He-gas pressure with the progress of transformation, and, indeed, such was observed. In order to maintain a constant pressure on the sample, we continuously regulated the gas pressure through a constant monitoring of the Manganin resistor.

## III. RESULTS

A typical example of the time development of the diffraction pattern observed after sudden application of pressure is shown in Fig. 1. The peak corresponding to the (110) reflection of the stable CsCl-type structure builds up while that of the (200) reflection of the metastable NaCl-type diminishes. The lattice constants of the NaCl and CsCl structures were measured to be about 7.27 and 4.37 Å, respectively, at a transition point. The fractional volume of the stable phase  $X(t)$  is given by

$$X(t) = \frac{I(t) - I(0)}{I(\infty) - I(0)} = \frac{I'(\infty) - I'(t)}{I'(\infty) - I'(0)}, \quad (1)$$

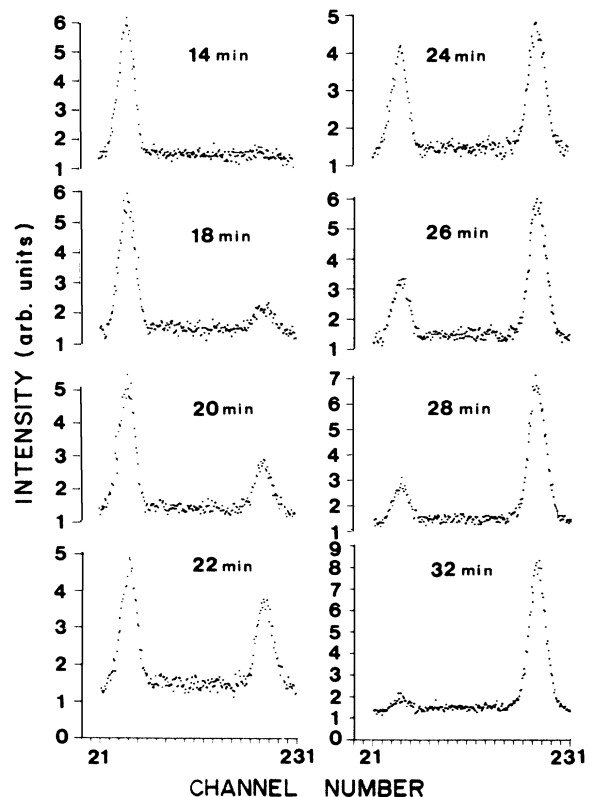


FIG. 1. Typical example of time sequence of the diffraction patterns of RbI during the transformation from the NaCl- to the CsCl-type structure. The horizontal axis is the channel number of the detector ( $0.04^\circ$  per channel). Note the change of scale of the vertical axis.

where  $I(t)$  [ $I'(t)$ ] are the integrated intensities of the stable (metastable) phase. The observed time developments of  $X(t)$  for various pressures at room temperature and at 240 K are summarized in Figs. 2(a) and 2(b), respectively. The values of pressure for each run are listed in Table II. Values of  $X(t)$  derived independently from  $I(t)$  and  $I'(t)$  agree to within 3%, which can be regarded as the absolute error of the measurements including both random and systematic errors. Simple inspection of Fig. 2(a) indicates that growth curves exhibit similar slope, except for the 7 and 9 growth curves which appear to have smaller slope. Note that those two curves were measured at pressures closest to  $P_c$  in the NaCl-to-CsCl transformation and the reverse one, respectively. We will show later that at room temperature most of growth curves are well represented by a scaling behavior derived from a simple model of nucleation and growth (although this is not the case for the 240-K data, as will be discussed later in more detail).

We may characterize the time scale of the transformation by defining the time at which the transformation has gone to half completion, i.e.,  $X(t_{1/2}) = \frac{1}{2}$ . The values of  $t_{1/2}$  in Table II were obtained from the analysis of the integrated intensities using Eq. (1). To obtain  $t_{1/2}$  over a wide pressure and temperature range, we carried out many quick searches, by monitoring Debye-Scherrer intensities of the high- and low-pressure phases on a storage video

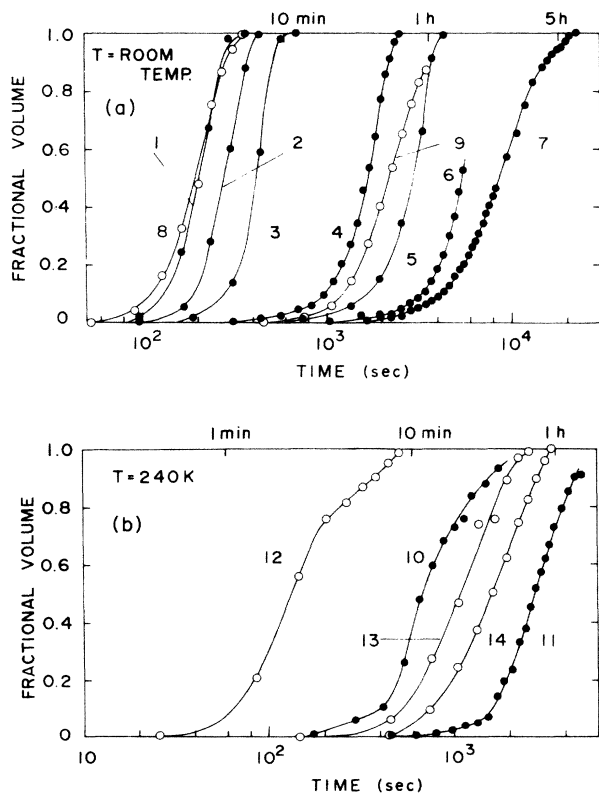


FIG. 2. Time dependence of the fractional volume of transformed region  $X(t)$  observed for various pressures at (a) room temperature and (b) at 240 K. Values of  $X(t)$  are plotted as solid circles for the NaCl-to-CsCl transformation and as open circles for the reverse transformation. The solid lines are guides for the eye.

TABLE II. Summary of the experimental conditions under which growth curves were observed and values of time,  $t_{1/2}$ , at which transformation has gone halfway to completion.

Direction of transformation	Run No.	Pressure (kbar)	$t_{1/2}$ (sec)
Room temperature			
B1 to B2	1	3.691	205
	2	3.691	280
	3	3.662	420
	4	3.634	1690
	5	3.620	2850
	6	3.613	5395
	7	3.606	8750
B2 to B1	8	3.197	200
	9	3.282	2200
240 K			
B1 to B2	10	4.255	666
	11	3.973	2730
B2 to B1	12	2.280	160
	13	2.562	1120
	14	2.632	1625

display.  $t_{1/2}$  was measured at the moment when the intensities of two peaks became approximately equal. Values of  $t_{1/2}$  measured by this method are presented as a function of pressure in Fig. 3. Although those values differ by up to 15% from the values obtained more carefully by using Eq. (1), it is clear from Fig. 3 that  $t_{1/2}(P)$  diverges as the pressure approaches  $P_c$  at all temperatures of this study, implying a thermal activation process is involved in the process of nucleation and growth. After 76 min at 200 K no transformation from the NaCl- to the CsCl-type structure had occurred by 5.67 kbar, the maximum pressure safely generated by the present apparatus. In Fig. 3 we find that at room temperature a pair of  $t_{1/2}$  curves, one for the NaCl-to-CsCl transformation and another for the reverse transformation, are located symmetrically around  $P \approx 3.45$  kbar. This pressure may be taken as an approximate  $P_c$  at room temperature. Also,  $P_c$  at 240 K is estimated to be about 3.34 kbar from the results of  $t_{1/2}$  listed in Table II.

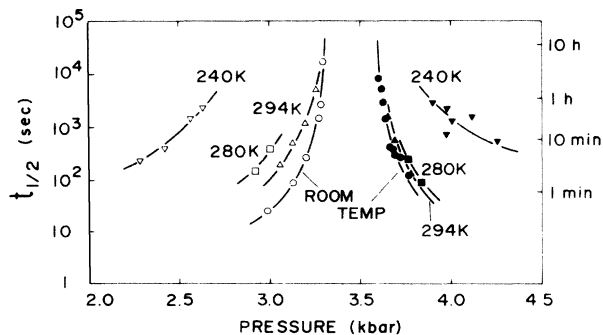


FIG. 3. Pressure dependence of  $t_{1/2}$  measured visually (see text). At any temperature  $t_{1/2}$  diverges as the pressure approaches  $P_c$ . The critical pressure is estimated to be about 3.45 kbar at room temperature.

## IV. ANALYSIS OF RESULTS

We begin by describing a simple picture of nucleation and growth at first-order phase transitions in solids originally due to Kolmogorov.<sup>5</sup> When the pressure is instantaneously changed beyond  $P_c$ , infinitesimal grains of stable phase are produced randomly within the sample at a constant rate,  $\Gamma$ , per unit volume. Although  $\Gamma(P, T)$  is time independent, the rate of effective nucleation decreases with time proportional to the fraction of metastable phase remaining,  $1 - X(t)$ . Once formed, a grain grows isotropically with constant domain-wall velocity  $v(P, T)$ . This is equivalent to the statement that the rate of volume growth of a grain is proportional to its free surface area. As a grain grows, it begins to impinge upon neighboring grains and finally ceases growing. Some scaling properties of this model are revealed directly from dimensional analysis. Since the model is completely characterized by two parameters  $\Gamma$  (with dimension  $t^{-1}L^{-d}$  in  $d$ -dimensional space) and  $v$  (dimension  $t^{-1}L$ ), it follows that there exists a single characteristic time scale and length scale given by

$$t_0 = (\Gamma v^d)^{-1/(d+1)}, \quad (2a)$$

and

$$\xi_0 = (v/\Gamma)^{1/(d+1)}, \quad (2b)$$

respectively. The time development of any quantity is universal when expressed in terms of the scaling time  $\tau = t/t_0$ . Similarly any quantity associated with spatial development (e.g., domain-size distribution function) is universal when expressed in a scaled length,  $\xi = l/\xi_0$ .

An explicit expression for the transformed volume fraction  $X(t)$  for this model was first given by Kolmogorov<sup>5</sup> and later independently by Avrami:<sup>6</sup>

$$X(t) = 1 - \exp \left[ -\Gamma \int_0^t V(t') dt' \right], \quad (3)$$

where  $V(t')$ , the volume occupied by a hypothetical "free" grain (one that does not impinge on a neighboring grain) at time  $t'$  after nucleation, is

$$V(t') = D(vt')^d, \quad (4a)$$

$$D = 2, \pi, 4\pi/3 \text{ for } d = 1, 2, 3. \quad (4b)$$

On substitution we have an expression similar to that found by Johnson and Mehl,<sup>7</sup>

$$X(t) = 1 - \exp \left[ -\frac{D}{d+1} \Gamma v^d t^{d+1} \right]. \quad (5)$$

This can be written in a universal form, which for  $d=3$  becomes

$$X(\tau) = 1 - \exp \left( -\frac{1}{3} \pi \tau^4 \right), \quad (6)$$

with  $\tau = t/t_0$  and  $t_0 = (\Gamma v^3)^{-1/4}$  in accordance with Eq. (2) for  $d=3$ . Note that the relation  $t_0 = 1.11t_{1/2}$  is obtained from  $X(t_{1/2}/t_0) = \frac{1}{2}$ . The value of  $t_{1/2}$  observed can therefore be interpreted as a measure of  $\Gamma v^3$  for the transformation process.

In order to compare the model with our experimental results, the room-temperature growth curves shown in

Fig. 2(a) are plotted as a function of the scaling time  $\tau$  in Fig. 4 along the theoretical scaled curve calculated by Eq. (6). It is seen in Fig. 4 that the theoretical curve is in good agreement with most of experimental data at room temperature. At the pressure closest to  $P_c$ , where  $t_{1/2}$  becomes very long, deviations from universal scaling appear. In particular, the scaling violation is obvious in growth process 7 with  $t_{1/2} \cong 143$  min. Among the various possibilities for this behavior, here we present two. The 7 growth curve was found to have a time exponent of 2.2 in Eq. (5). Cahn<sup>13</sup> suggested that when the new phase nucleates on grain surfaces, grain edges, or grain corners, the growth curve shows, respectively,  $t$ ,  $t^2$ , or  $t^3$  dependence in the later stage. A noninteger value of 2.2 may be expected when various types of nucleation sites are active. It is possible that at  $P$  closest to  $P_c$ , the heterogeneous nucleation mechanisms predominate over the homogeneous nucleation which we have assumed in our model. This speculation is consistent with the observation by Daniels and Skoultchi<sup>9</sup> that for single-crystal RbI the surface layers transform at lower pressure than does the interior. The decrease in time exponent at  $P$  close to  $P_c$  has been also reported on polycrystalline KCl.<sup>10</sup> Another possibility is the effect of a finite critical droplet size,  $r_c$ . Nuclei redissolve or grow according to whether their radius is less than or greater than  $r_c$ . We have thus far assumed  $r_c \cong 0$ . The modification of Eq. (6) to include a finite  $r_c$  has been discussed by Ishibashi and Takagi,<sup>14</sup> who find

$$X(\tau) = 1 - \exp \left[ -\frac{\pi}{3} [(\tau + \tau_c)^4 - \tau_c^4] \right], \quad (7)$$

with  $\tau_c = r_c/vt_0$ . Since the formulation now includes two characteristic times,  $t_0$  and  $r_c/v$ ,  $X(\tau)$  is no longer universal. The dashed curve in Fig. 4 is obtained by the choice  $\tau_c = 0.35$ . If this interpretation is correct the observed value of  $\tau_c$  indicates that the critical droplet size is already comparable to the average domain size at, say,  $t = t_{1/2}$  for  $P$  close to  $P_c$ .

The scaling formula derived from the simple model of nucleation and growth has been successfully used to inter-

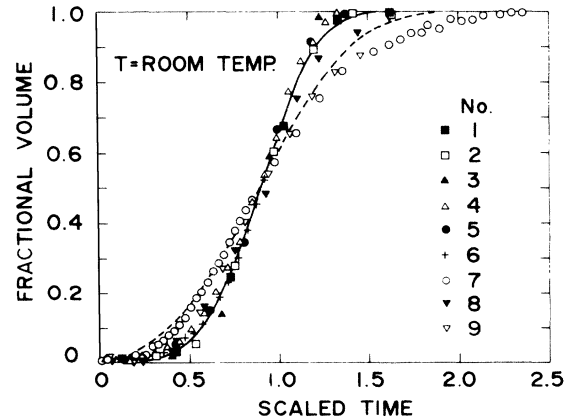


FIG. 4. The scaled curve of  $X(t)$  plotted in terms of the scaled time  $\tau = t_{1/2}/t_0$ . The solid line is the curve of  $X(t)$  calculated by Eq. (6). The dashed line is the calculation when  $\tau_c = 0.35$  (see text).

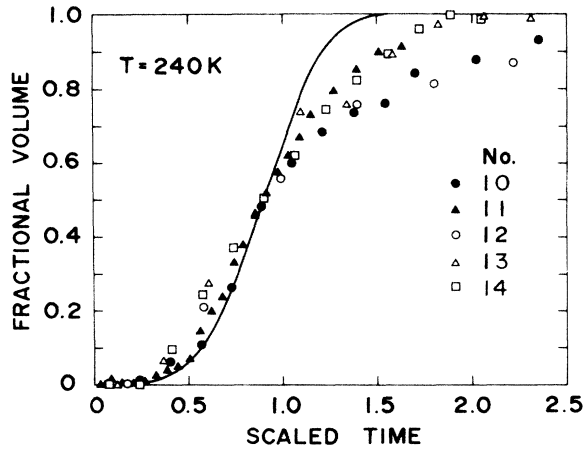


FIG. 5. The scaled curve of  $X(t)$  for 240 K. The experimental data deviate from the theoretical curve calculated by Eq. (6) (solid line), the largest deviation occurring at the pressures farthest from  $P_c$  (10 and 12).

pret the time development of  $X(t)$  observed at room temperature. The results for 240 K, however, are not described by this scaling formula (Fig. 5). The time exponent  $n$  obtained from the fit of the growth curves in Fig. 2(b) to Eq. (5) showed rather complicated behavior: In the early growth stage  $n = 2.3$ – $3.5$ , while in the late stage  $n = 0.8$ – $2.3$ . That is, not only is the time exponent considerably smaller than the postulated value of  $n = 4$ , but the growth curves do not fall onto a universal curve. Moreover, it should be noted in Fig. 5 that the largest deviation, corresponding to the smallest value of time exponent, occurs at the highest pressure for the NaCl-to-CsCl transformation and at the lowest pressure for the reverse transformation. The behavior at 240 K is clearly different from that observed at room temperature where the scaling violation was found at the pressure closest to  $P_c$ . Later we will discuss a possible origin of the scaling violation at low temperature.

We tried to analyze the observed divergent behavior of the characteristic time  $t_0$  against the excess pressure  $\Delta P$

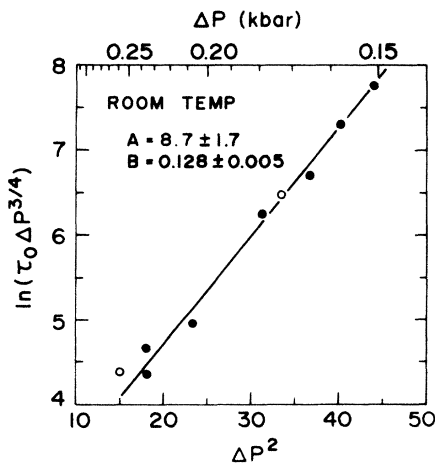


FIG. 6. Observed characteristic time  $t_0 (= 1.11t_{1/2})$  plotted versus  $\Delta P^{-2} = (P - P_c)^{-2}$  with  $P_c = 3.455$  kbar. The solid line is a least-squares fit with Eq. (8) to the observed values.

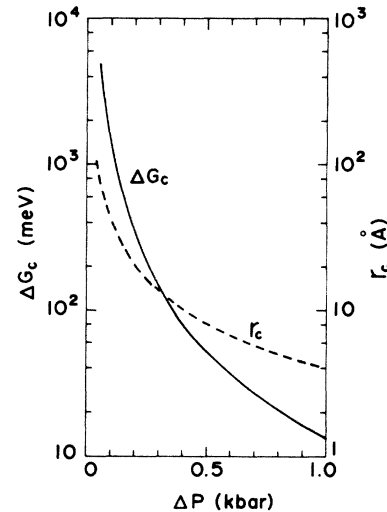


FIG. 7. Estimated thermodynamic energy barrier for nucleation  $\Delta G_c$  and critical droplet radius  $r_c$  plotted against  $\Delta P$ . The observations were carried out in the range of  $0.151 \leq \Delta P \leq 0.258$  kbar.

( $= |P - P_c|$ ) based on classical nucleation and growth theory summarized in the Appendix. According to the theoretical expression given in Eq. (A8),  $t_0$  observed at room temperature were fitted to

$$t_0(\Delta P) = A (\Delta P)^{-3/4} \exp[B(\Delta P)^{-2}], \quad (8)$$

where parameters  $A$  and  $B$  are defined in the Appendix. This form gives good description of the room-temperature results with  $A = 8.7 \pm 1.7$  sec kbar $^{3/4}$ ,  $B = 0.128 \pm 0.005$  kbar $^{-1}$ , and  $P_c = 3.455$  kbar as shown in Fig. 6. We notice that since the constant  $K_1$  in Eq. (A4) is determined from the value of  $B$ , we can estimate the thermodynamic energy barrier for nucleation  $\Delta G_c(\Delta P)$  and the critical droplet radius  $r_c(\Delta P)$ . The results are presented in Fig. 7. Note that in the very narrow region of  $0.151 \leq P \leq 0.258$  kbar where the observations were carried out,  $\Delta G_c$  decreases from 0.58 to 0.20 eV, which corresponds to increase in nucleation rate by  $10^6$ , while  $r_c$  changes from 27 to 16 Å. We did not analyze the 240-K data because the growth process at 240 K seems to be more complicated than that assumed in our model.

## V. DISCUSSION

The present measurements at room temperature agree completely with the results reported in our previous paper,<sup>11</sup> and are represented by the simple model of nucleation and growth. This model, however, failed to describe the new results for low temperature. We are aware of the modest nature of the model assumptions. It is, for example, by no means clear that  $\Gamma(P, T)$  and  $v(P, T)$  both are independent of time.

An important process which may give rise to time dependence of the domain-wall velocity  $v$  at first-order phase transformations in solids is the slow relaxation of the internal stresses produced in the vicinity of domain walls by a volume difference between the two structures. The effect of the internal stress on the domain-wall veloci-

ty has been found to exist at the temperature-induced phase transformation in tin.<sup>15</sup> The effect of elastic strain can be taken into account within the framework of the present treatment as follows: Since the elastic strain energy  $\epsilon$  created by the formation of the stable phase increases proportionally to the volume of this stable phase, we should replace  $\Delta G$  in Eqs. (A1) and (A6) by  $\Delta G + \epsilon$ . One immediately notices that the nucleation rate and the growth velocity are very sensitive to  $\epsilon$  as well as  $\Delta G$ . On the other hand, the internal stresses relax with time through the processes involving the movement of dislocations. We therefore expect that the rate of growth of domain walls may become time dependent when the strain energy  $\epsilon$  is comparable to  $|\Delta G|$  and the rate of stress relaxation is slower than the rate of growth.

We roughly estimated the relevant energies. From Eq. (A3)  $\Delta G$  is estimated to be  $-8.1$  meV/molecule for  $\Delta P=1$  kbar. Assuming that both phases are elastically isotropic and that the interface between the nucleated domain and the matrix is coherent,  $\epsilon$  can be estimated by the macroscopic theory of elasticity using the sphere-in-hole model:<sup>16</sup>

$$\epsilon = \left[ \frac{2K\mu}{3K+4\mu} \right] \frac{(\Delta V)^2}{\bar{V}}, \quad (9)$$

where  $K$  is the bulk modulus of the domain of the stable phase,  $\mu$  is the shear modulus of the metastable matrix phase,  $\Delta V$  is the difference in volume per molecule between the two structures, and  $\bar{V}$  is the averaged volume of two structures per molecule. Substituting  $K=16$  GPa,<sup>17</sup>  $\mu=2.62$  GPa,<sup>18</sup>  $\Delta V=12.9$  Å<sup>3</sup>/molecule, and  $\bar{V}=89.7$  Å<sup>3</sup>/molecule, we obtain  $\epsilon$  to be 16.6 meV/molecule. This value may be regarded as the maximum estimate because  $\epsilon$  will be smaller in the incoherent interface than in the coherent interface. It is difficult to estimate the rate of relaxation. Experimentally, however, it is known that in LiF the dislocation velocity increases by about  $10^5$  with increasing temperature from 200 to 300 K.<sup>19</sup> If a similar situation occurs in RbI, it is not unreasonable that the rate of stress relaxation increases drastically with temperature and its time scale becomes negligibly small in comparison with the characteristic time of transformation at room temperature.

From these considerations we suggest the following picture of the transformation process. The strain energy  $\epsilon$  of RbI is comparable to  $|\Delta G|$ . At room temperature, however, the stress is relaxed much faster than the rate of growth, thus resulting in a constant domain-wall velocity given by  $v \propto 1 - \exp[\Delta G/(k_B T)]$ . At 240 K the stress relaxation time becomes much larger and the strain energy is gradually accumulated as the growth of domains proceeds. Hence the velocity becomes slower in the later stage of growth process:

$$v(t) \propto 1 - \exp\{[\Delta G + \epsilon(t)]/(k_B T)\}.$$

These interpretations are qualitatively consistent with the following experimental results. (1) At room temperature, the transformation process satisfies the scaling rule which is derived based on simple assumption that the nucleation rate and the domain-wall velocity both are independent of

time. (2) At 240 K, within a single growth process the deviation of the observed values from the simple scaling curve becomes more evident in the later stage of the transformation. (3) Comparing different processes, the deviation is found to increase as  $\Delta P$  increases (that is, as the characteristic time of transformation becomes shorter).

Finally, we comment on our results of measurements attempting to observe time development of the average domain size  $\bar{R}(t)$ . The time development of  $\bar{R}(t)$  is given for our model by

$$\bar{R}(t) = \xi_0 \left[ \frac{X(t)}{\int_0^t \exp(-\frac{1}{3}\pi t'^4) dt'} \right]^{1/3} \quad (10)$$

for  $d=3$ . Therefore the observation of  $\bar{R}(t)$  permits evaluation of  $\xi_0$ , which, together with  $t_0$ , gives the value of  $\Gamma$  and  $v$  separately through Eqs. (2a) and (2b). This was the motivation for attempting to measure  $\bar{R}(t)$ . It is possible to observe  $\bar{R}(t)$  by a diffraction method if the average size of domains is small enough to yield the broadening of diffraction peaks beyond the instrumental resolution. Since no broadening of diffraction peaks was detected by the use of the area detector having momentum resolution of  $0.031$  Å<sup>-1</sup>, we carried out another neutron diffraction experiment with the identical sample using a triple-axis spectrometer with a higher resolution of  $0.007$  Å<sup>-1</sup>. However, we could not find a clear indication of the line broadening within the experimental errors. The temporal resolution of this experiment ( $\cong 7$  min) was lower than that using the area detector ( $\cong 30$  sec) and did not allow investigation of the early phase of growth.

#### ACKNOWLEDGMENTS

This research was supported in part by the Division of Basic Energy Sciences, U.S. Department of Energy, under Contract No. DE-AC02-76CH00016, and carried out as part of the Japan-U.S. Cooperative Neutron Scattering Program (No. 8413).

#### APPENDIX

We examine the pressure and temperature dependence of the characteristic time  $t_0$  in the framework of the classical nucleation and growth theory.<sup>20</sup> Since  $t_0 = (\Gamma v^3)^{-1/4}$  in our model, we have to investigate the  $P$  and the  $T$  dependence of  $\Gamma$  and  $v$ . To begin with, we assume that a spherical nucleus is formed homogeneously in the matrix phase, and that the transformation strain energy is negligible. The energy of nucleation consists of two competitive energy terms, a volume-energy term which tends to favor nucleation, and a surface-energy term which tends to prevent it. Then the thermodynamic energy barrier for nucleation,  $\Delta G_c$ , is found to be

$$\Delta G_c = \frac{16\pi}{3} \frac{\sigma^3}{(\Delta G)^2}, \quad (A1)$$

at a critical radius  $r_c$  of nucleus

$$r_c = \frac{2\sigma}{|\Delta G|}, \quad (A2)$$

where  $\sigma$  is the interfacial energy and  $\Delta G$  is the free-energy difference between the metastable (initial) phase and the stable phase. At constant temperature,  $\Delta G$  can be approximated near  $P_c$  by

$$\Delta G \cong \Delta V \Delta P, \quad (\text{A3})$$

where  $\Delta V$  is the volume change caused by the transformation and  $\Delta P$  is the excess pressure beyond  $P_c$ ,  $\Delta P = P - P_c$ . For the NaCl-to-CsCl transformation in RbI,  $\Delta V$  was found to be  $-12.9 \text{ \AA}^3/\text{molecule}$  and thus  $\Delta G = -8.1 \Delta P$  (in kbar) meV/molecule. Substituting Eq. (A3) into Eq. (A1), we obtain  $\Delta G_c(\Delta P)$ :

$$\Delta G_c = K_1 (\Delta P)^{-2} \quad (\text{A4})$$

with  $K_1 = 16\pi\sigma^3/3(\Delta V)^2$ . Turnbull and Fisher<sup>21</sup> derived the following expression for the steady-state nucleation  $\Gamma$  in condensed systems:

$$\Gamma = N \left[ \frac{k_B T}{h} \right] \exp \left[ -\frac{\Delta G_c + Q}{k_B T} \right], \quad (\text{A5})$$

where  $N$  is the number of nucleation sites per unit volume,  $k_B$  is Boltzmann's constant,  $h$  is Planck's constant, and  $Q$  is the activation energy needed for a molecule to cross the interface between two phases.

On the other hand, the growth velocity  $v$  is given in

terms of  $Q$  and  $\Delta G$  by<sup>20</sup>

$$v = \lambda \left[ \frac{k_B T}{h} \right] \exp \left[ -\frac{Q}{k_B T} \right] \left[ 1 - \exp \left[ \frac{\Delta G}{k_B T} \right] \right], \quad (\text{A6})$$

where  $\lambda$  is the thickness of the interface. For small degree of metastability,  $\Delta G \ll k_B T$ , we have

$$v \cong \left[ \frac{\lambda}{h} \right] (-\Delta G) \exp \left[ -\frac{Q}{k_B T} \right]. \quad (\text{A7})$$

In the present case the above approximation holds within the precision of 1% up to  $\Delta P = 0.5$  kbar. On substitution we finally obtain  $t_0(\Delta P, T)$  as

$$\begin{aligned} t_0(\Delta P, T) &= (\Gamma v^3)^{-1/4} \\ &= K_2 T^{-1/4} \exp \left[ \frac{Q}{k_B T} \right] |\Delta P|^{-3/4} \\ &\quad \times \exp \left[ \frac{K_1}{4k_B T (\Delta P)^2} \right], \end{aligned} \quad (\text{A8})$$

where  $K_2 = h(Nk_B\lambda^3 |\Delta V|^3)^{-1/4}$ . The dominant  $\Delta P$  dependence of  $t_0$  is given by the last factor in Eq. (A8), thus  $t_0$  diverges as  $\exp[B(\Delta P)^{-2}]$  when  $P \rightarrow P_c$ .

<sup>1</sup>For a recent review, see J. D. Gunton, M. San Miguel, and P. S. Sahni, in *Phase Transitions and Critical Phenomena*, edited by C. Domb and J. L. Lebowitz (Academic, London, 1983), Vol. 8.

<sup>2</sup>The earlier references are quoted in Ref. 1. F. F. Abraham, S. W. Koch, and R. C. Desai, *Phys. Rev. Lett.* **49**, 923 (1982); T. Ohta, D. Jasnow, and K. Kawasaki, *ibid.* **49**, 1223 (1982); M. Grant and J. D. Gunton, *Phys. Rev. B* **28**, 5496 (1983).

<sup>3</sup>S. Katano and M. Iizumi, *Phys. Rev. Lett.* **52**, 835 (1984); S. Komura, K. Osamura, H. Fujii, and T. Takeda, *Phys. Rev. B* **30**, 2994 (1984).

<sup>4</sup>D. G. Morris, F. M. Besag, and R. E. Smallman, *Philos. Mag.* **29**, 43 (1974); T. Hashimoto, K. Nishihara, and Y. Takeuchi, *J. Phys. Soc. Jpn.* **45**, 1127 (1978); Y. Noda, S. Nishihara, and Y. Yamada *ibid.* **53**, 4241 (1984).

<sup>5</sup>A. N. Kolmogorov, *Bull. Acad. Sci. U.S.S.R., Phys. Ser.* **3**, 555 (1937).

<sup>6</sup>M. Avrami, *J. Chem. Phys.* **7**, 1103 (1939); **8**, 212 (1940); **9**, 177 (1941).

<sup>7</sup>W. A. Johnson and R. F. Mehl, *Trans. Am. Inst. Min. Metall. Pet. Eng.* **135**, 416 (1939).

<sup>8</sup>A. Lacam, J. Peyronneau, and J. L. Kopystynski, *J. Phys. (Paris)* **35**, 287 (1974); L. D. Livshitz, Y. N. Ryabinin, L. V. Larinov, and A. S. Zverev, *Zh. Eksp. Teor. Fiz.* **55**, 1173 (1968) [*Sov. Phys.—JETP* **28**, 612 (1969)]; E. F. Skelton, S. B. Qadri, A. W. Webb, C. W. Lee, and J. P. Kirkland, *Rev. Sci.*

*Instrum.* **54**, 403 (1983).

<sup>9</sup>W. B. Daniels and A. I. Skoultchi, *J. Phys. Chem. Solids* **27**, 1247 (1966).

<sup>10</sup>N. Hamaya and S. Akimoto, *High Temp. High Pressures* **13**, 347 (1981).

<sup>11</sup>Y. Yamada, N. Hamaya, J. D. Axe, and S. M. Shapiro, *Phys. Rev. Lett.* **53**, 1665 (1984).

<sup>12</sup>J. A. Leake, W. B. Daniels, J. Skalyo, B. C. Frazer, and G. Shirane, *Phys. Rev.* **181**, 1251 (1969).

<sup>13</sup>J. W. Cahn, *Acta Metall.* **4**, 449 (1956).

<sup>14</sup>Y. Ishibashi and Y. Takagi, *J. Phys. Soc. Jpn.* **31**, 506 (1971).

<sup>15</sup>R. G. Wolfson, M. E. Fine, and A. W. Ewald, *J. Appl. Phys.* **31**, 1973 (1960).

<sup>16</sup>J. D. Eshelby, in *Solid State Physics*, edited by F. Seitz and D. Turnbull (Academic, London, 1956), Vol. 3, p. 79.

<sup>17</sup>K. Asaumi, T. Suzuki, and T. Mori, *Phys. Rev. B* **28**, 3529 (1983).

<sup>18</sup>M. Ghafelehbashi, D. P. Dandekar, and A. L. Ruoff, *J. Appl. Phys.* **41**, 652 (1970).

<sup>19</sup>J. J. Gilman and W. G. Johnston, in *Solid State Physics*, edited by F. Seitz and D. Turnbull (Academic, London, 1962), Vol. 13, p. 147.

<sup>20</sup>For example, D. Turnbull, in *Solid State Physics*, edited by F. Seitz and D. Turnbull (Academic, London, 1956), Vol. 3, p. 225.

<sup>21</sup>D. Turnbull and J. C. Fisher, *J. Chem. Phys.* **17**, 71 (1949).